PLANE-STRAIN COMPRESSION OF ALUMINUM CRYSTALS*

W. F. HOSFORD, Jr.†

A plane-strain compression test was used to investigate the work-hardening of aluminum crystals deforming by multiple slip. Shear stress–strain curves were constructed from the compression data with an analysis of Bishop and Hill. The curves fall in a narrow band, indicating that, under conditions of multiple slip, the basic shear stress for slip depends primarily on the amount of prior slip, and that the combination of active slip systems is of much less importance. This observation supports a basic assumption in several theories of polycrystalline flow.

Lattice rotation during plane-strain compression are reported and compared with similar observations during rolling.

DEFORMATION PLANAIRE EN COMPRESSION DE CRISTAUX D'ALUMINIUM

A l'aide d'essais de compression en déformation planaire, l'auteur a étudié le durcissement de déformation de cristaux d'aluminium après déformation par glissement multiple.

Les courbes tension de cisaillement—déformation ont été construites à partir des résultats des essais de compression par la méthode d'analyse de Bishop et Hill.

Les courbes se situent dans une bande étroite indiquant que dans le cas des glissements multiples la tension fondamentale de cisaillement dépend d'abord de l'importance du glissement antérieur et que la combinaison des systèmes de glissements actifs présente beaucoup moins d'importance. Ces observations appuient une hypothèse de base énoncée dans de nombreuses théories de déformation des polycristaux.

On a observé des rotations réticulaires au cours des essais de compression. Elles sont comparées à des observations similaires après laminage.

EBENE KOMPRESSION VON ALUMINIUMKRISTALLEN

Die Verfestigung von Aluminiumkristallen durch Verformung auf Grund von Vielfachgleitung wurde in Kompressionsversuchen mit ebener Verformung untersucht. Aus einer Analyse der Kompressionsdaten nach Bishop und Hill wurden Verfestigungskurven konstruiert. Die Kurven ligen innerhalb eines engen Bandes, was darauf hindeutet, daß unter den Bedingungen für Vielfachgleitung die wesentliche Schubspannung für Gleitung in erster Linie von der Größe der Vorabgleitung abhängt und daß die Kombination aktiver Gleistsysteme von sekundärer Bedeutung ist. Diese Beobachtung stützt eine grundlegende Annahme in einer Reihe von Theorien des polykristallinen Fließens.

Es wird über eine Gitterdrehung während der ebenen Kompression berichtet. Sie wird mit ähnlichen Beobachtungen während des Walzens verglichen.

INTRODUCTION

In 1938 Taylor[1,2] analyzed the deformation of a randomly oriented f.c.c. polycrystal and related the shape of the tensile stress–strain curve for a polycrystal to that of the shear stress–strain curve of a single crystal of the same material. Later Bishop and Hill[3,4] developed a simpler analysis on somewhat firmer grounds, leading to the same results. Recently these analyses have been extended to crystallographically textured metals, forming the basis for texture hardening predictions.[5] It is therefore important that the limitations of the underlying theory be examined.

One of the critical assumptions in these works is that when a crystal deforms by slip on many slip systems, the shear stress necessary to continue slip is the same for all slip systems and depends only on the total shear strain on all of the slip systems. This assumption implies that the shear stress–strain (τ versus γ) curves are identical for all orientations of crystals. Certainly this assumption appears unrealistic in view of the fact that in tension tests, some orientations of single crystals undergo extensive easy glide, while other orientations exhibit little or no glide. However, since the grains in a polycrystalline sample must deform by the simultaneous operation of five or more slip systems, this assumption need hold only for such conditions of multiple slip.

Traditionally, studies of single crystal deformation have been largely limited to uniaxial tension or compression testing. Only when the stress axis is aligned with [111] or [001] can more than two slip systems be activated simultaneously. Kocks[6] studied "polyslip" in aluminium crystals with tension tests of these orientations as well as two combined stress tests. He found a considerable divergence of the τ versus γ curves after a shear strain of about 0.05, with the [111] curve the highest. Although six or eight slip systems were stressed equally in these tests, not all of these systems were active. At least three slip systems, and probably six, operate in a [111] oriented crystal, but in a [001] crystal, slip becomes locally restricted to two systems after the first few per cent strain.[7]

In another study,[8] aluminum crystals of various

* Received July 22, 1965.

† Department of Chemical and Metallurgical Engineering, The University of Michigan, Ann Arbor, Michigan.

orientations were forced to undergo axially symmetric flow by drawing them through conical dies. Although the results were in reasonable agreement with the theory, there was a considerable amount of scatter which was attributed to the nonhomogeneity of flow through the dies.

Because enforced plane-strain seemed to offer a simpler method of activating various combinations of slip systems, a program of plane-strain deformation of aluminum single crystals was undertaken. Since the initiation of this program, a similar study has been made by Chin *et al.*[9] on permalloy crystals.

EXPERIMENTAL PROCEDURE

Oriented single crystals were grown from high purity aluminum in the form of strips with a uniform rectangular cross section of $\frac{1}{8}$ in. $\times$ $\frac{7}{8}$ in. for about $4\frac{1}{2}$ in. of their length. The technique involved directional solidification of a seeded blank in a solid graphite boat. Ten crystals were grown; nine were of highly symmetrical orientations (two had the same orientation), and one was a non-symmetrical orientation which resulted when the seeding failed. The orientations were checked by Laue back-reflection photographs; the nominal orientations and the divergence from these are given in Table 1. Here the specimen axes are designated x, y and z, with x as the normal to the flat surface (the axis of subsequent compression), z as the length of the crystal (axis of extension), and y as the width direction (axis of zero strain). The divergence from the nominal orientation is described by three angles, α, β and γ, which designate the clockwise rotations of the nominally aligned crystal axes about the y, z and x axes, respectively. In addition, a polycrystalline specimen was prepared by annealing a strip cut from a rolled sheet $2\frac{1}{2}$ hr at 375°C.

Testing was done in an Instron machine with a plane-strain fixture similar to that described by Ford.[10] The crystal was placed between a pair of flat carbide indentors of $\frac{1}{8}$ in. thickness, which overlapped the crystal (Fig. 1). A 0.002 in. Teflon film between the indentors and the crystal provided lubrication. The crystals were indented at 8–10 locations along their length, under a series of varying loads. At each indentation, the remaining thickness, h, was subsequently measured with a micrometer and the true compressive strain was calculated as

$$\varepsilon = \ln (ho/h) \tag{1}$$

where ho was the initial thickness ($\sim$0.125 in.) at that location. For each indentation the true compressive stress was taken to be

$$\sigma = P/wt \tag{2}$$

Where P was the indentation load, w, the crystal width ($\frac{7}{8}$ in.), and t, the indentor width ($\frac{1}{8}$ in.).

Laue back-reflection photographs were taken on many of the indentations to determine the lattice rotation during the plane-strain compression.

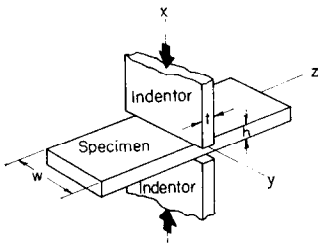

FIG. 1. Schematic illustration of the plane-strain compression set-up. When the specimen is compressed by the flat indentations, the unloading regions adjacent to the plastic zone prevent lateral spreading along y, so that $\varepsilon_y = 0$ $\varepsilon_z = -\varepsilon_x$.

TABLE 1. Crystal orientations

Crystal number	Nominal orientation		Angles of divergence from nominal orientation in degrees		
	(x)	$[z]$	α	β	γ
1	(111)	[11$\bar{2}$]	-1	$+\frac{1}{2}$	-1
2	(110)	[11$\bar{2}$]	1	$+1$	$-1\frac{1}{2}$
3	(100)	[011]	$-2\frac{1}{2}$	$+4$	0
4	(1$\bar{1}$0)	[110]	$+\frac{1}{2}$	$-1\frac{1}{2}$	$1\frac{1}{2}$
5	(1$\bar{1}$0)	[111]	$-1\frac{1}{2}$	$-\frac{1}{2}$	0
6	(11$\bar{2}$)	[111]	$-\frac{1}{2}$	$+2\frac{1}{2}$	1
7	(1$\bar{1}$0)	[111]	$-\frac{1}{2}$	$+\frac{1}{2}$	0
8	(15, 2, 5)	[1, 10, $\bar{1}$]			
9	(111)	[1$\bar{1}$0]	$-\frac{1}{2}$	$+\frac{1}{2}$	-2
10	(100)	[100]	0	$+2$	0

ANALYSIS OF STRESS–STRAIN DATA

True compressive stress–strain curves are shown in Fig. 2. A great deal of orientation dependence is evident; the curve for crystal 4, (1$\bar{1}$0) [110], is more than twice as high as those for several others. It is necessary to reduce these curves to a shear stress–strain (τ versus γ) basis to determine whether the orientation dependence is due solely to differences in the amounts of slip required to produce the imposed shape change, as assumed, or whether some of the orientation dependence also results from differing rates of work-hardening.

The Bishop and Hill analysis[3,4] was used for converting the compressive stress–strain (σ versus ε) data to crystallographic shear stress and strain (τ and γ). This analysis is based on considering the work per unit volume, dw, associated with producing an increment of normal strain. Since this work is expended om the slip systems,

$$dw = \sum_i \tau_i \, d\gamma_i \tag{3}$$

which reduces to

$$dw = \tau \, d\gamma \tag{4}$$

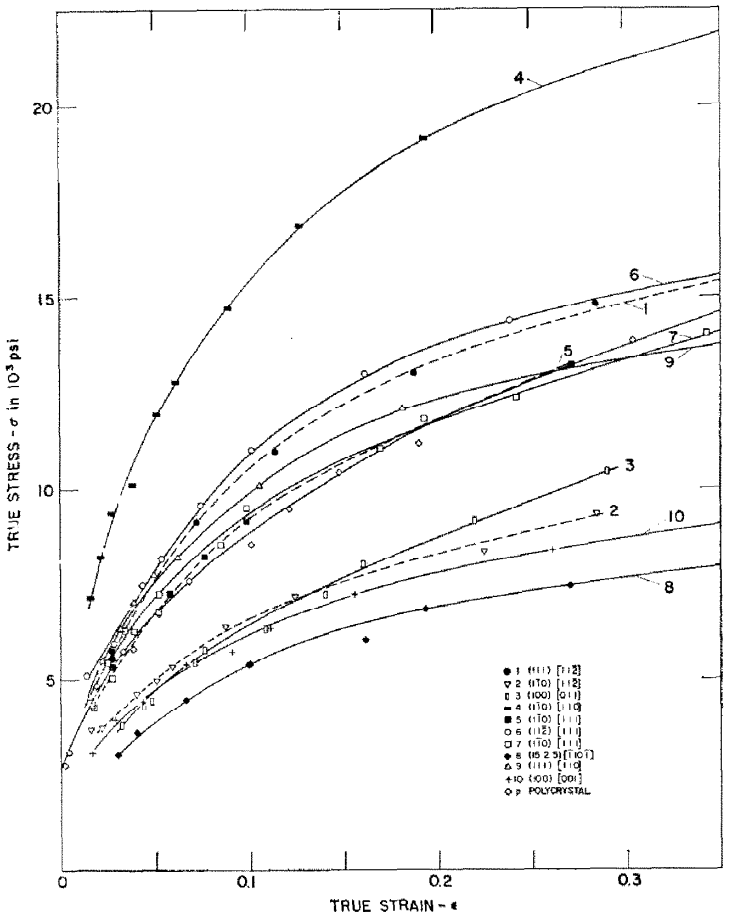

FIG. 2. True stress–strain curves for plane strain compression, showing experimental points.

if τ, the stress necessary to produce slip, is the same on all active systems. Here $d\gamma$ denotes $\sum_i |d\gamma_i|$. If, as in these experiments, all of the mechanical work is supplied by the action of a single applied stress, σ_x, dw is also given by

$$dw = \sigma_x \, d\varepsilon_x \tag{5}$$

Combining (4) and (5) and defining $M = dw/\tau \, d\varepsilon_x$

$$M = \sigma_x/\tau = d\gamma/d\varepsilon_x \tag{6}$$

For a given shape change, the external strains, $d\varepsilon_y$, $d\varepsilon_z$, $d\varepsilon_{yz}$, $d\varepsilon_{zx}$ and $d\varepsilon_{xy}$ are fixed relative to $d\varepsilon_x$. Ideally for plane-strain, $d\varepsilon_z = -d\varepsilon_x$, $d\varepsilon_y = 0$ and $d\varepsilon_{yz} = d\varepsilon_{zx} = d\varepsilon_{xy} = 0$. For a particular crystal orientation, the angles between the cubic crystal axes 1, 2 and 3 are known relative to the specimen axes x, y and z, and the stresses may therefore be expressed relative to the 1, 2, 3 axes. Then, M may be expressed as

$$M = \frac{dw}{\tau \, d\varepsilon_x} = \frac{1}{\tau \, d\varepsilon_x}[\sigma_1 \, d\varepsilon_1 + \sigma_2 \, d\varepsilon_2 + \sigma_3 \, d\varepsilon_3 + 2\sigma_{23} \, d\varepsilon_{23} + 2\sigma_{31} \, d\varepsilon_{31} + 2\sigma_{12} \, d\varepsilon_{12}] \tag{7}$$

A substitution of

$$A = \sigma_2 - \sigma_3, \; B = \sigma_3 - \sigma_1, \; F = \sigma_{23}, \; G = \sigma_{31}, \text{ and } H = \sigma_{12}$$

simplifies equation (7) to

$$M = 1/\tau \, d\varepsilon_x[-B \, d\varepsilon_1 + A \, d\varepsilon_2 + 2F d\varepsilon_{23} + 2G \, d\varepsilon_{31} + 2H \, d\varepsilon_{12}] \tag{8}$$

Bishop and Hill[3] showed that only certain combinations of values for A through H result in stress states which can activate five or more slip systems. These are shown in Table 2, together with the slip systems activated. (The axis and slip system designations are described in Fig. 3.) According to the principle of maximum virtual work, the appropriate combination of A through H in equation (8) is the one that results in the largest value of M.

The M values calculated in this way are listed in Table 3, together with the Bishop and Hill stress states and active slip systems. For several orientations two stress states lead to the same maximum M. In these cases the active slip systems are those common to both stress states.

TABLE 2. Bishop and Hill stress states and slip systems

	Stress-values of						Operating slip systems (sign denotes direction of operation; 0 denotes non-operation)											
	A	B	C	F	G	H	aI	aII	aIII	bI	bII	bIII	cI	cII	cIII	dI	dII	dIII
1	1	−1	0	0	0	0	+	−	0	+	−	0	+	−	0	+	−	0
2	0	1	−1	0	0	0	0	+	−	0	+	−	0	+	−	0	+	−
3	−1	0	1	0	0	0	−	0	+	−	0	+	−	0	+	−	0	+
4	0	0	0	1	0	0	0	+	−	0	−	+	0	+	−	0	−	+
5	0	0	0	0	1	0	−	0	+	+	0	−	+	0	−	−	0	+
6	0	0	0	0	0	1	+	−	0	+	−	0	−	+	0	−	+	0
7	½	−1	½	0	½	0	0	−	+	+	−	0	+	−	0	0	−	+
8	½	−1	½	0	−½	0	+	−	0	0	−	+	0	−	+	+	−	0
9	−1	½	½	½	0	0	−	+	0	−	0	+	−	+	0	−	0	+
10	−1	½	½	−½	0	0	−	0	+	−	+	0	−	0	+	−	+	0
11	½	½	−1	0	0	½	+	0	−	+	0	−	0	+	−	0	+	−
12	½	½	−1	0	0	−½	0	+	−	0	+	−	+	0	−	+	0	−
13	½	0	−½	½	0	½	+	0	−	+	−	0	0	+	−	0	0	0
14	½	0	−½	−½	0	½	+	−	0	+	0	−	0	0	0	0	+	−
15	½	0	−½	½	0	−½	0	+	−	0	0	0	+	0	−	+	−	0
16	½	0	−½	−½	0	−½	0	0	0	0	+	−	+	−	0	+	0	−
17	0	−½	½	0	½	½	0	−	+	+	−	0	0	0	0	−	0	+
18	0	−½	½	0	−½	½	+	−	0	0	−	+	−	0	+	0	0	0
19	0	−½	½	0	½	−½	−	0	+	0	0	0	+	−	0	0	−	+
20	0	−½	½	0	−½	−½	0	0	0	−	0	+	0	−	+	+	−	0
21	−½	½	0	½	½	0	−	+	0	0	0	0	0	+	−	−	0	+
22	−½	½	0	−½	½	0	−	0	+	0	+	−	0	0	0	−	+	0
23	−½	½	0	½	−½	0	0	+	−	−	0	+	−	+	0	0	0	0
24	−½	½	0	−½	−½	0	0	0	0	−	+	0	−	0	+	0	+	−
25	0	0	0	½	½	−½	−	+	0	0	0	0	+	0	−	0	−	+
26	0	0	0	½	−½	½	+	0	−	0	−	+	−	+	0	0	0	0
27	0	0	0	−½	½	½	0	−	+	+	0	−	0	0	0	−	+	0
28	0	0	0	½	½	½	0	0	0	+	−	0	0	+	−	−	0	+

For the polycrystalline specimens, M was taken as 3.30, the value derived by Bishop and Hill[4] for randomly oriented f.c.c. polycrystals undergoing plane-strain. (A somewhat higher value of 3.53 has been derived[5] from the von Mises yield criterion and Taylor's factor of $M = 3.06$ for randomly oriented f.c.c. polycrystals under uniaxial tension. The Bishop and Hill value, however, gives a better fit with the present data.

After testing the indentations were examined to determine whether plane-strain conditions did prevail Lateral spreading along y was greatest in crystal 4, $(1\bar{1}0)$ [110], where the average lateral strain, ε_y, was estimated to be about 20% of the compressive strain, ε_x. In all other crystals, ε_y amounted to considerably less than 10% of ε_x. The relatively large spreading in the $(1\bar{1}0)$ [110] orientation is explained by the high constraining stress, $\sigma_y = \sqrt{6}\tau$, necessary to maintain zero spreading. At the ends of the indentation σ_y must vanish. Here the lack of constraint lowers M from $2\sqrt{6}$ to $\sqrt{6}$ locally.

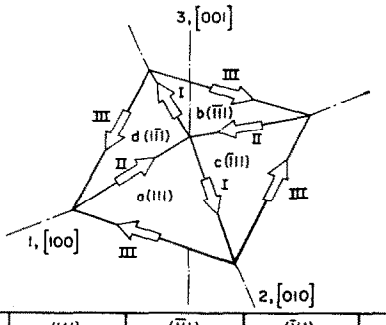

PLANE	(111)			(1̄11)			(1̄11)			(11̄1)		
DIRECTION	011	101	110	011̄	101	1̄10	011̄	101	110	011̄	1̄01	110
SYSTEM	a_1	a_2	a_3	b_1	b_2	b_3	c_1	c_2	c_3	d_1	d_2	d_3

FIG. 3. Half-octahedron representing slip systems in an f.c.c. crystal. Each face is a {111} slip plane and each edge a ⟨011⟩ slip direction. The axis and slip system designation used throughout are indicated.

Examination of the indentations also revealed macroscopic shearing of some crystals. In fact, the testing techniques, employed here, does not insure that ε_{yz}, ε_{zx} and ε_{xy} be zero as assumed. For some crystals the symmetry of the orientation prevented macroscopic shears. Where shearing was observed, the orientation lacked such symmetry and a simple analysis indicated that the imposed shape change could be accommodated with less slip (lower M) if macroscopic shearing did occur. For these orientations the M values were calculated and the active slip systems determined for the relaxed strain conditions. These latter values, indicated with an asterisk in Table 3, were used in the data analysis.

TABLE 3. Orientation factors and slip systems

Crystal no.	Orientation x	z	$M/\sqrt{6}$	Stress state	Slip systems
1	(111)	$[11\bar{2}]$	$\frac{3}{2}$	−24, 28	$b_1, -b_2, -c_3, +d_3$
2	(110)	$[11\bar{2}]$	$\frac{4}{3}$	−6, 25	$-a_1, a_2, c_1, -d_2$
			*1		$*c_1, -d_2$
3	(100)	[011]	1	4, −2	$-a_2, b_3, -d_2, d_3$
4	$(1\bar{1}0)$	[110]	2	6	$a_1, -a_2, b_1, -b_2, -c_1, c_2, -d_1, d_2$
5	$(1\bar{1}0)$	[111]	$\frac{5}{3}$	−6	$-a_1, a_2, -b_1, b_2, c_1, -c_2, d_1, -d_2$
			*$\frac{3}{2}$		$*-b_1, -c_2, +d_1$
6	$(11\bar{2})$	[111]	$\frac{3}{2}$	24, −28	$-b_1, +b_2, +c_3, -d_3$
7	$(1\bar{1}0)$	[111]	Same as 5		
8	(15, 2, 5)	[1, 10, $\bar{1}$]	1.19	−24	$b_1, -b_2, c_1, -c_2, -d_2, d_3$
			*0.946		$*d_3, -b_2, -d_2$
9	(111)	[110]	$\frac{5}{3}$	6	$a_1, -a_2, +b_1, -b_2, -c_1, -c_2, -d_1, d_2$
			*$\frac{3}{2}$		$*b_1, -b_2, c_2, -d_1$
10	(100)	[001]	1	1, −2	$-a_2, -b_2, -c_2, -d_2$
	Polycrystal		1.35		

* Values with finite shear strains ε_{yz}, ε_{xz} and ε_{xy}.

SHEAR STRESS–STRAIN CURVES

Shear stress–strain curves were constructed from the compressive stress–strain data by taking

$$\tau = \sigma/M \tag{9}$$

and

$$\gamma = M\varepsilon \tag{10}$$

These equations neglect the effects of any lattice rotation that might have occurred during the test.

The shear stress–strain curves for the single crystals and the polycrystal fall into a single band (Fig. 4). This clustering indicates that different combinations of active systems produce similar rates of work hardening as long as several systems are active. It should be noted that in half of the crystals (numbers 1, 2, 5, 7 and 9) there should be no slip systems in critical relationship (90° Burgers' vectors). We can conclude that the formation of sessile −90° jogs by dislocation intersection is not necessary for work hardening since these crystals harden at approximately the same rate as the others. A similar conclusion can be made about the formation of Lomer–Cottrell barriers by interaction of dislocations on systems of conjugate relationship, since the curve for crystal 10 which had no active systems in conjugate relationship was not significantly different from the rest.

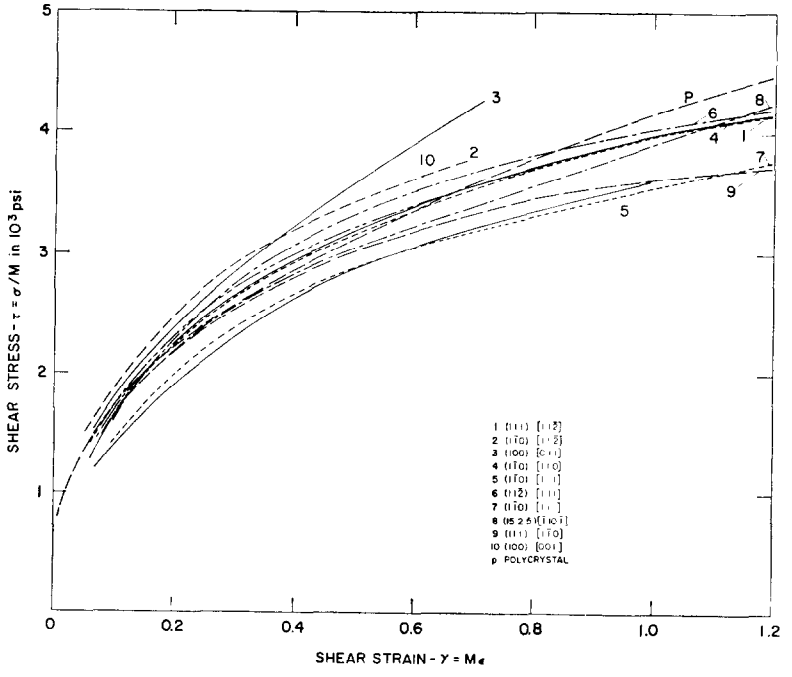

FIG. 4. Shear stress–strain curves constructed from Fig. 3 by taking $\tau = \sigma/M$ and $\gamma = M\varepsilon$. Experimental points are omitted for clarity.

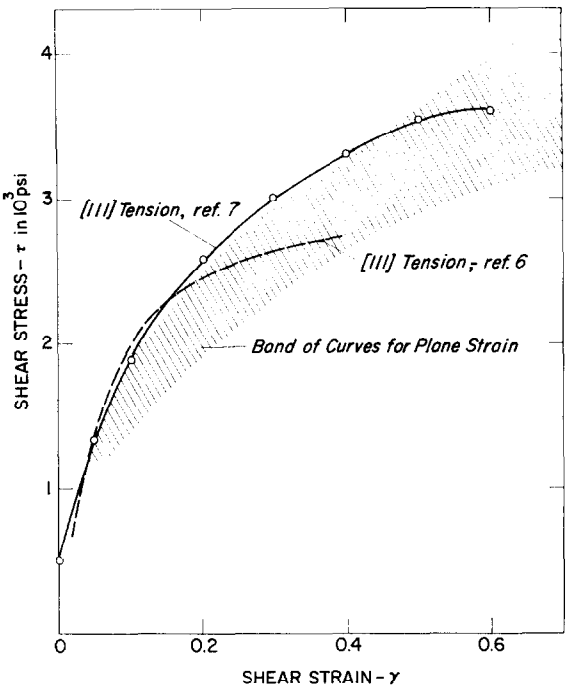

FIG. 5. Comparison of shear strain curves for [111] crystals in tension with the band of curves determined by plane-strain compression.

Since a [111] oriented single crystal extended in tension undergoes multiple slip, its shear stress–strain curves should be comparable with those reported. In Fig. 5, it may be seen that two published curves for [111] aluminum crystals extended in tension came close to falling in band of the present curves. In making such a comparison, it is important to estimate the effect of friction in the plane-strain tests, since this would be absent in tension tests. This can be done with a simple slab analysis. If the Teflon film is assumed to have a constant shear strength τ_0, then

$$\bar{\sigma} - \sigma_0 = \frac{\tau_0 t}{2h} \tag{11}$$

where $\bar{\sigma}$ is the average compressive stress and σ_0 is the true flow stress. $\bar{\sigma} - \sigma_0$ represents the amount of elevation of the curves by the frictional constraint. The ratio of the indentor width, t, to the specimen thickness, h, rises from 1 to 1.5 as the reduction is increased to 33%. Taking τ_0 as 1000 psi (the tensile yield stress is about 2000 psi[11]). $\bar{\sigma} - \sigma_0$ would increase from 500 to 750 psi. Hence the τ versus γ curve for a crystal of $M = 2.5$ is raised by about 200–300 psi by the frictional constraint. If the stress–strain band determined by this work were lowered by this approximate correction, the [111] tensile stress–strain curves would still lie in or slightly above the band. This indicates that similar work-hardening characteristics prevail in both tension and plane-strain compression, as expected.

The significant conclusion is that for aluminum crystals deforming by slip on several systems, strain hardening depends primarily on the total amount of slip on all systems, with relatively little dependence upon which combinations of slip systems are active. Chin *et al.*[9] have reached a similar conclusion about strain hardening in permalloy (4% Mo, 17% Fe, 79% Ni) crystals deformed in plane-strain. This conclusion justifies the basic assumption in the Taylor, and Bishop and Hill analyses.

LATTICE ROTATION

Since the M factors depend on orientation, they would be expected to change with any lattice rotation accompanying indentation. Whether such orientation changes contribute appreciably to the spread in the τ versus γ curves could best be determined by measuring the lattice rotation. It was hoped that such measurements might also contribute to the understanding of texture development in plane-strain working operations such as sheet rolling.

Laue back-reflection photographs were made of three or four indentations in each crystal. Some of the X-ray results are shown in Fig. 6. Here the approximate outlines of the blurred reflections from low indice planes are plotted in the central portion of a Wulff net, together with the sharp spots from undeformed regions. The shape and size of the reflections indicate the axis and degree of local rotation, while the displacement of the reflections indicate the general lattice rotation.

Several types of lattice rotation are apparent in Fig. 6. In many cases the orientations change can be described as a simple rotation about the y-axis (which would correspond to the transverse direction in rolling).

In crystal 1, (111) [11$\bar{2}$], there is a relatively large local and general rotation about y. The sense of the rotation is in agreement with the observations of Brick and Williamson[12] on rolled α-brass crystals. They found that a (111) [11$\bar{2}$] crystal adopted a (110) [001] orientation after an 80% reduction.

For crystal 6, (11$\bar{2}$) [111], the asterism smaller, but there appears to be a small rotation about y, it is not clear whether the additional rotation about z is real or due to slight misalignment during subsequent X-rays. Brick and Williamson[12] reported that this orientation was stable in α-brass up to 80% reduction, but rotated toward (110) [112] at 99% reduction.

The Laue photographs of crystal 10, (100) [001] indicate a large amount of asterism and general

FIG. 6 (a–i). Lattice rotations indicated by Laue back-reflection photographs of indented regions. The blurred reflections from low indice planes are plotted in the central portion of a Wulff net, together with sharp spots from undeformed regions.

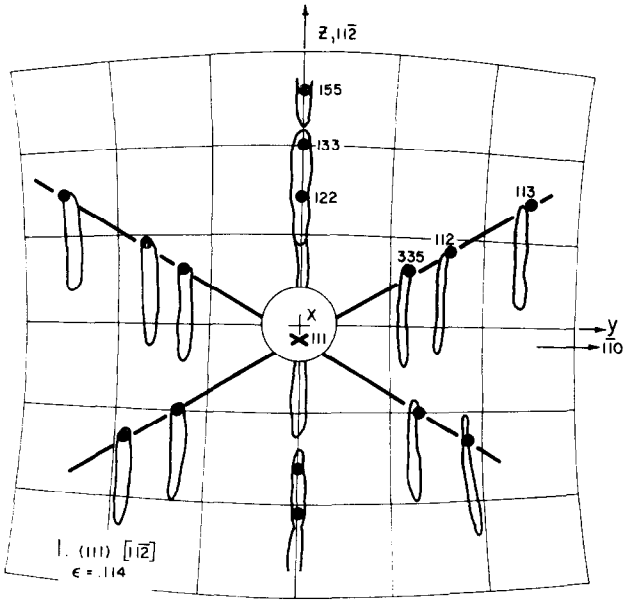

FIG. 6 (a)

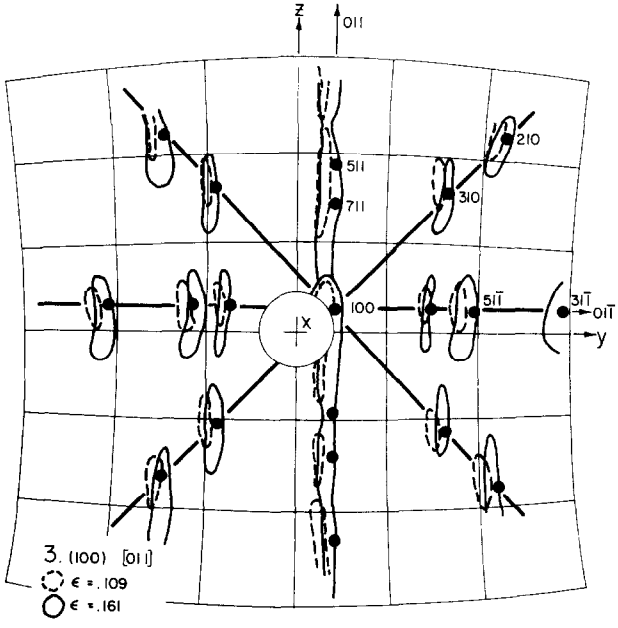

FIG. 6 (c)

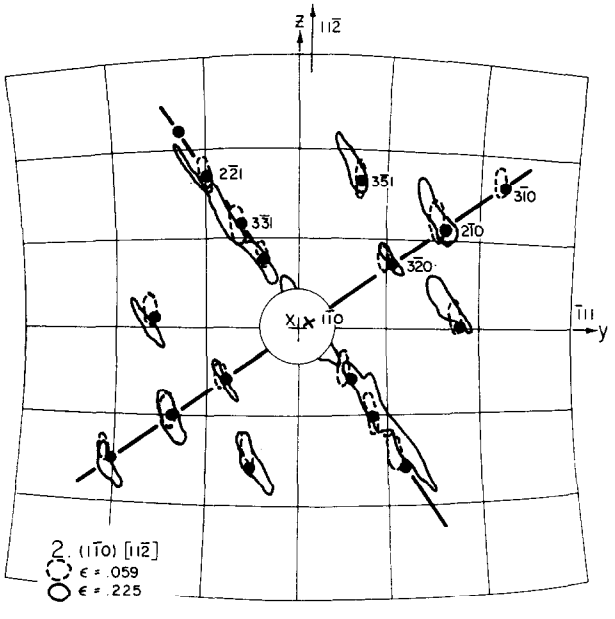

FIG. 6 (b)

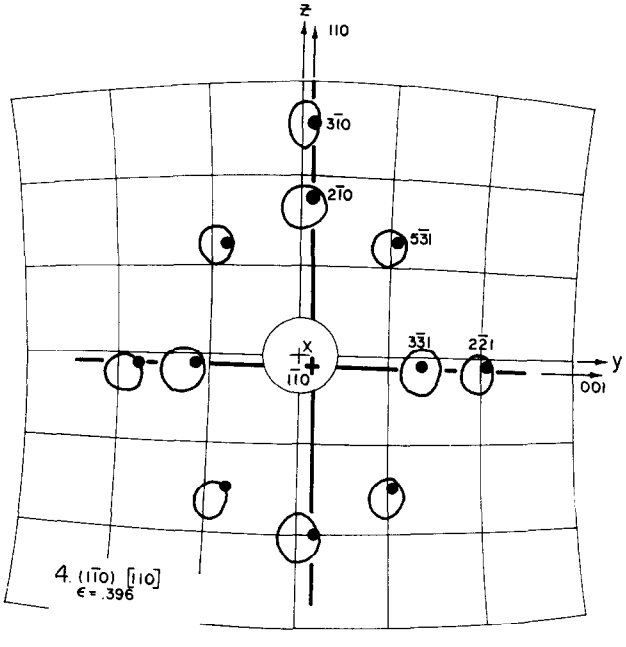

FIG. 6 (d)

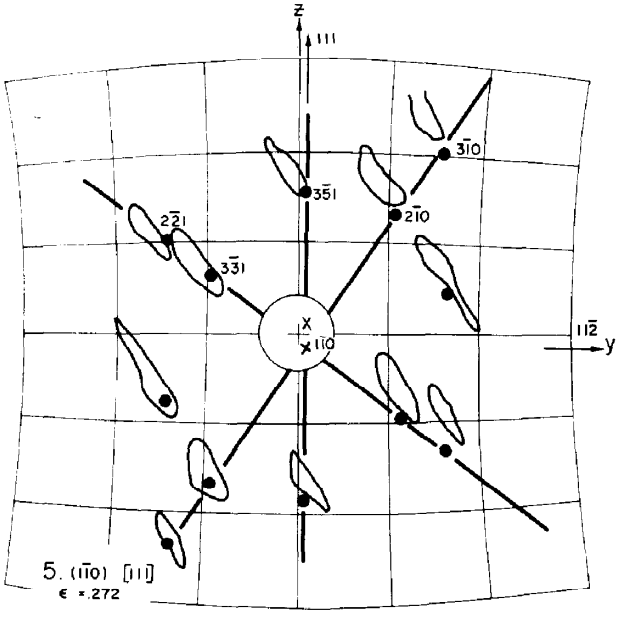

FIG. 6 (e)

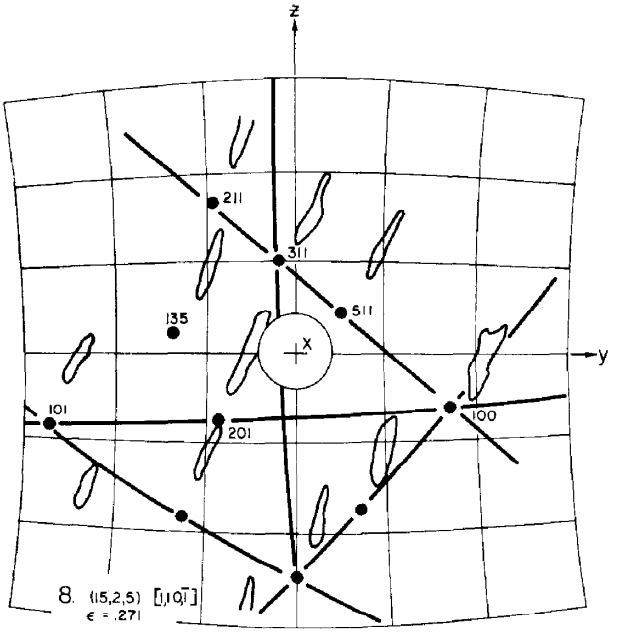

FIG. 6 (g)

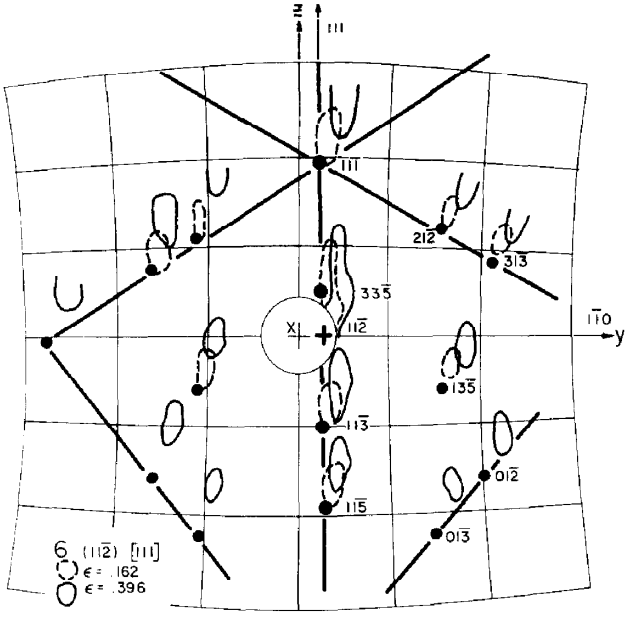

FIG. 6 (f)

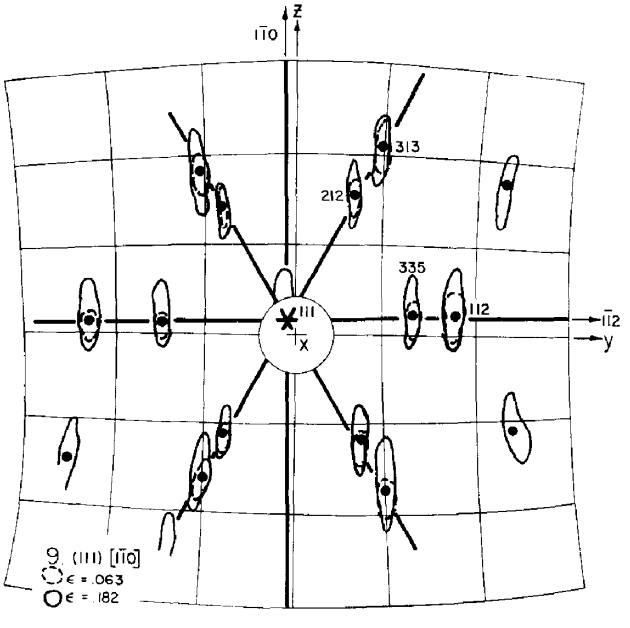

FIG. 6 (h)

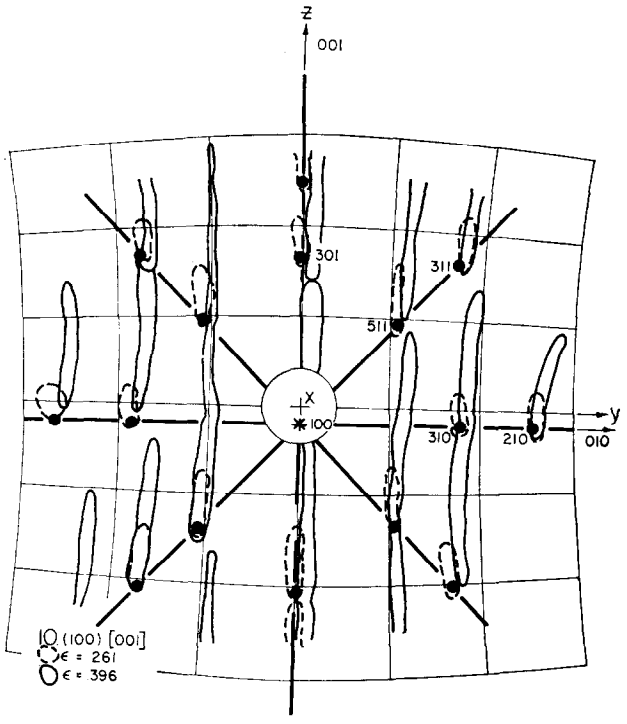

FIG. 6 (i)

rotation about y. Although Fig. 6 shows only one sense of rotation, the opposite sense was observed in still another Laue picture. Barrett and Steadman[13] found that a copper crystal of this orientation fragmented into (100) [001] plus (135) [21$\bar{1}$] orientations after a 98% rolling reduction. The rotations observed here, however, would not lead to the latter orientation.

For both crystals 3 and 9, (100)[011] and (111)[1$\bar{1}$0] the asterism indicates a moderate local rotation about y, but no general rotation is apparent.

Crystal 4, (1$\bar{1}$0)[110], was unique in that there was neither a general rotation nor a directionality to the asterism. Furthermore the asterism was quite small, the circular reflection being only about $3\frac{1}{2}°$ in dia. at a true strain of 0.152 and about $4\frac{1}{2}°$ in dia. at a strain of 0.396. The stability of this orientation is quite surprising in view of its high strength. Chin *et al.*[9] report that a (1$\bar{1}$0)[110] oriented permalloy crystal underwent severe deformation banding during plane-strain compression. Slip line traces in one of their photomicrographs suggest an orientation change of about 30° in the deformation bands. They observed that this orientation work hardened less rapidly than the others at high strains and attributed the lower hardening rate to a decrease of the effective M value by deformation banding. Deformation banding was not observed in the present work though the stress–strain curves may have been lowered somewhat by a loss of plane-strain constraint at the ends of the indentations.

The simplicity of the rotations reported above is not surprising. Except for crystal 9, all of the orientations have mirror symmetry about the x–z plane, so no general rotation about z or x should be expected. However, a freedom to undergo a macroscopic shear, ε_{zx}, may have increased the general rotation of some of the crystals about y.

The remaining orientations lacked mirror symmetry about the x–z plane and underwent macroscopic shears ε_{yz}. Consequently the rotations observed are not directly comparable with rotations during rolling. At low strains the asterism generally indicates a local rotation about an axis oriented near y, but at higher strains the axis of rotation shifts increasingly away from y. This shift is apparent in the plot for crystal 2, (1$\bar{1}$0)[11$\bar{2}$], where the axis approaches [110] at the higher strain. For crystal 5, (1$\bar{1}$0)[111], the rotation axis lies near [11$\bar{1}$] at a strain of 0.272, and some general rotation is observed. Crystal 7, which had the same orientation, behaved similarly. For crystal 8, the axis of rotation was near [$\bar{1}$1$\bar{1}$] and the mean orientation was approximately (301)[010] after a strain of 0.271.

The lattice rotations were small enough so that corresponding M changes amounted to only a few per cent. Therefore, little of the divergence of the τ versus γ curves can be attributed to this cause.

CONCLUSIONS

The orientation dependence of strength of aluminum crystals under plane-strain compression is consistent with the analyses of Taylor and Bishop and Hill, and supports the basic assumption that the shear stress for slip depends primarily on the amount of prior slip; the combination of active slip systems being much less important. This agreement strengthens the basis of predicting "texture hardening" effects in f.c.c. metals by this type of crystallographic analysis.

ACKNOWLEDGMENTS

This work was initiated at the Massachusetts Institute of Technology, with the support of the U.S. Atomic Energy Commission Contract No. AT(30-1)-1310. The author wishes to thank B. C. Wonsiewicz for help with the crystal growth and testing, and W. A. Backofen for encouragement and helpful criticism. The aluminum was supplied by the Aluminum Company of America.

The analysis of results, lattice rotation measurements, and writing were done at the University of Michigan with the support from U.S. Army Research

Office—Durham under Contract No. DA-31-124-ARO-D-321. E. W. Kelley and G. Y. Chin read and criticized the manuscript.

REFERENCES

1. G. I. Taylor, *Stephen Timoshenko 60th Anniversary Volume*, p. 218. Macmillan, N.Y. (1938).
2. G. I. Taylor, *J. Inst. Metals* **62,** 307 (1938).
3. J. F. W. Bishop and R. Hill, *Phil. Mag.* **42,** 51 (1951).
4. J. F. W. Bishop and R. Hill, *Phil. Mag.* **42,** 1298 (1951).
5. W. F. Hosford, Jr. and W. A. Backofen, *Fundamentals of Deformation Processing*, edited by W. A. Backofen *et al.*, p. 259. Syracuse U. Press, Syracuse (1964).
6. U. F. Kocks, *Acta Met.* **8,** 345 (1960).
7. W. F. Hosford, Jr., R. L. Fleischer and W. A. Backofen, *Acta Met.* **8,** 187 (1960).
8. W. F. Hosford, Jr., *Trans. Met. Soc. A.I.M.E.* **233,** 329 (1965).
9. G. Y. Chin, E. A. Nesbitt and A. J. Williams, *Acta Met.* **14,** 467 (1966).
10. H. Ford, *Proc. Inst. mech. Engrs* **159,** 115 (1948).
11. *J. Teflon*, **5,** 4 (1964).
12. R. M. Brick and M. A. Williamson, *Trans. Am. Inst. Min. metall. Engrs* **143,** 84 (1941).
13. C. S. Barrett and F. W. Steadman, *Trans. Am. Inst. Min. metall. Engrs* **147,** 57 (1942).